Revealing the reversible rotation of magnetization in exchange-coupled composite media switching

Thomas Hauet, S.H. Florez, D Margulies, Y Ikeda, B Lengsfield, N Supper, K Takano, O Hellwig, B. D. Terris

Revealing the reversible rotation of magnetization in exchange-coupled composite media switching

T. Hauet,[a] S. Florez, D. Margulies, Y. Ikeda, B. Lengsfield, N. Supper, K. Takano, O. Hellwig, and B. D. Terris
San Jose Research Center, Hitachi Global Storage Technologies, 3403 Yerba Buena Rd., San Jose, California 95135, USA

(Received 31 August 2009; accepted 8 November 2009; published online 3 December 2009)

We present a study of the magnetic reversal mechanism for exchange coupled composite perpendicular media, i.e., hard granular layer/exchange-coupling layer (ECL)/soft layer (SL) systems, without soft underlayer. Using a vibrating sample magnetometer, the out-of-plane and in-plane components of the magnetization are monitored simultaneously, while sweeping an external out-of-plane magnetic field. The in-plane signal reveals the reversible rotation of the magnetization during the switching process. The amplitude of this rotation is correlated with the variations in coercivity and angular dependence of the remanent coercivity for different ECL and SL thicknesses. © *2009 American Institute of Physics*. [doi:10.1063/1.3270535]

One of the main challenges currently faced by the hard disk drive industry is maintaining both writability and magnetic stability within magnetic volumes so small that the magnetic anisotropy energy responsible for stabilizing the direction of the magnetization becomes comparable to the energy of thermal fluctuations at room temperature. While for single layer perpendicular media, writability and stability are correlated through the magnetocrystalline anisotropy, it has been demonstrated in recent years that adding a soft magnetic layer (SL) to the usual hard granular layer (HL), in a so-called exchange-coupled composite (ECC) media can improve the writability-to-stability ratio.[1,2] Theoretical models have been developed for the proposed incoherent reversal process in ECC media[3,4] and several experimental demonstrations of the advantages of ECC media with respect to recording performance have been published.[5–9] Most of these reports focus on defining optimum properties for the SL as well as for the interfacial exchange-coupling between the HL and the SL. However, only a few experiments have been performed for the purpose of understanding the fundamental nature of the incoherent reversal or confirming the theoretical predictions in actual perpendicular media structures.

Here we study an ECC system grown without a soft underlayer (SUL) in order to investigate the incoherent reversal process. The absence of the SUL and the use of a vibrating sample magnetometer (VSM) to sense both the out-of-plane and in-plane component of the magnetization simultaneously, allows observing and quantifying the tilt of the SL magnetization during the field induced reversal. We prepared a series of samples with different SL thicknesses in order to study the effect of SL thickness on the degree of magnetization tilt in the ECC system. Finally, we demonstrate the origin of the "reversibility" observed during the minor loop analysis reported in previous experiments.[7,10,11]

Multiple ECC structures with no SUL have been deposited onto 65-mm-diameter glass disks at room temperature using a dc magnetron sputtering system. A 30-nm-thick seed multilayer contains a NiW layer as well as two successive Ru layers deposited under high and then low sputtering pressure. The hard granular magnetic layer (HL), namely $CoPtCr-SiO_x$ (14 nm) has a saturation magnetization of $M_s=550$ emu/cm^3 and an anisotropy field of $H_{kHL}=14$ kOe. Different CoRu exchange-coupling layer (ECL) thicknesses have been deposited from 0 to 3 nm. For the SL, we use a highly exchange-coupled CoPtCrB alloy, i.e., with a strong coupling between the grains, which is very different from the magnetically isolated grains in the HL. The SL thickness has been varied from 0 to 10 nm with $M_s=350$ emu/cm^3. All ECC media have been finally covered with an overcoat for protection against oxidation. A commercial DMS VSM, including a rotating magnetic field and two pairs of fixed pickup coils at 90° with respect to each other, was used to measure the components of the magnetization both perpendicular-to-the-plane of the sample (M_{pp}) and in-

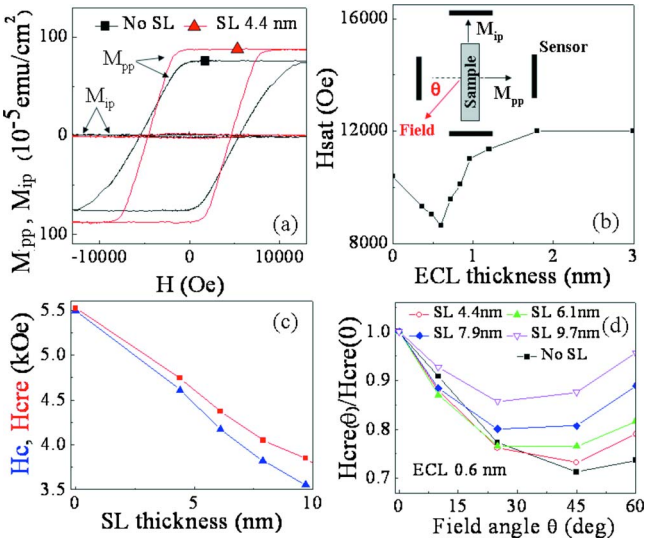

FIG. 1. (Color online) (a) Out-of-plane (M_{pp}) and in-plane (M_{ip}) components of the magnetization as a function of external magnetic field for samples with no SL and 4.4 nm SL. (b) Saturation field as a function of ECL thickness. The inset in (b) sketches the VSM measurement setup. (c) Coercivity H_c and remanent coercivity H_{cr} as a function of SL thickness. (d) Remanent coercivity as a function of field angle for different samples with SL thicknesses varied from 0 to 9.7 nm.

[a]Electronic mail: thomas.hauet@lpm.u-nancy.fr.

plane (M_{ip}), as described in the inset of Fig. 1. All the measurements were performed at room temperature.

Figure 1(a) shows M_{pp} and M_{ip} for a single HL and an ECC structure with 0.6 nm ECL and 4.4 nm SL. During this measurement, the field has been applied perpendicular-to-the-plane and swept between −15 and 15 kOe. In all figures, we plot the moment per area for direct comparison of all different samples. As expected from previous theoretical[1,3] and experimental studies,[7,12] the ECC structure has a higher nucleation field (H_n), lower saturation field (H_{sat}), lower coercive field (H_c), and narrower switching field distribution as compared to the single HL granular media. In Fig. 1(b), we present the evolution of H_{sat} as a function of the ECL thickness, i.e., as a function of the interlayer exchange coupling amplitude. The lowest H_{sat} is found for an ECL thickness of 0.6 nm. Indeed for a very strong coupling, the HL and SL magnetization reverse coherently, so that the magnetic properties are those of a laminated system (at least for small thicknesses of the SL). For a very weak coupling, the HL and SL magnetization reverse almost independently. Therefore, only an intermediate coupling allows optimizing the specific degree of reversal incoherency that is needed to create an additional torque from the SL onto the HL.[8]

For all following samples, we use a 0.6 nm thick ECL. Figure 1(c) shows H_c and the remanent coercivity (H_{cr}) as a function of the SL thickness. H_c and H_{cr} are continuously decreasing as the SL thickness increases. This behavior is often explained by an increasing influence of the torque induced by the SL onto the HL.[7,10] In other words, as the SL thickness increases, the evolving difference of H_c and H_{cr} originates from a more incoherent and thus more reversible switching process.[10,11] Figure 1(d) shows the angular dependence of the normalized H_{cr} for different SL thicknesses. For the pure HL sample (i.e., no SL), the curve has a minimum at 45° with $H_{cr}(45°)/H_{cr}(0°)$ around 0.7. The difference between this value and the pure Stoner–Wohlfarth model that applies for isolated grains may originate from multiple sources, such as intergranular exchange coupling within the HL, magnetocrystalline anisotropy dispersion of the grains or thermal effects.[5,7] As the SL thickness increases, one can observe a systematic increase in the $H_{cr}/H_{cr}(0°)$ minimum value as well as a decrease in the field angle where the minimum occurs. These evolutions reflect the increase in reversal incoherency due to both an increased lateral exchange coupling and an increased torque of the SL on the HL.[5–7]

The above results confirm that we have grown ECC samples without SUL that show a magnetic behavior identical to previously published reports.[5–9] However, so far no direct measurement of the "reversible" tilting of the SL magnetization has been reported yet. One way to measure this effect directly is to monitor the in-plane moment (M_{ip}), while measuring the usual M_{pp} out-of-plane hysteresis loop. Nevertheless, in Fig. 1(a), no significant M_{ip} signal is observed when applying the field along the perpendicular direction. This absence of any M_{ip} signal originates from the distribution of anisotropy axes in the SL and HL. The full width at half maximum of the x-ray rocking curve, which measures the c-axis misalignment of the magnetic grains, is typically of the order of 3° for our ECC structures. Such a distribution induces different in-plane directions of rotation for the SL moments over the 25 mm^2 sample area, resulting in an average M_{ip} signal close to zero over the entire field range.

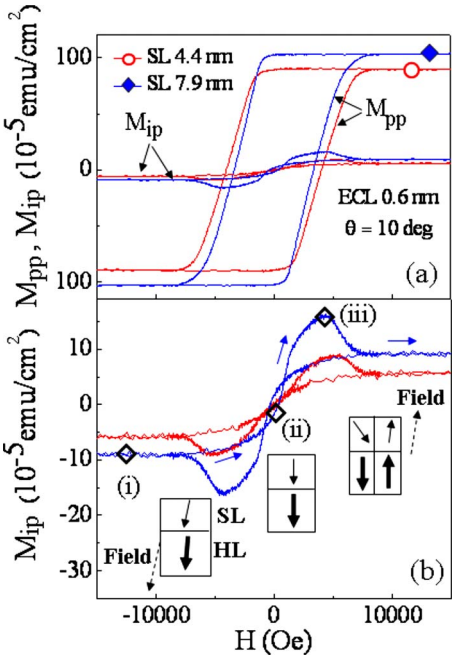

FIG. 2. (Color online) (a) Out-of-plane (M_{pp}) and in-plane (M_{ip}) components of the magnetization as a function of external magnetic field for samples with 4.4- and 7.9-nm-thick SL. (b) Expanded view of the M_{ip} signal. The open diamonds in (b) indicate the positions (i), (ii), and (iii) that correspond to the sketches of the magnetization of the two layers within the ECC structure.

To break the symmetry of all in-plane directions, we performed the same measurement, as in Fig. 1(a), with an external field applied at 10° tilt with respect to the average perpendicular anisotropy axis. The result of this experiment is presented in Fig. 2(a) for SL thicknesses of 4.4 and 7.9 nm, both with a 0.6 nm ECL. A clear in-plane component appears whose amplitude reaches a maximum around the coercive field and increases as the SL thickness increases. Figure 2(b) shows a more detailed expanded view of the in-plane component in Fig. 2(a). At −12 kOe (i), the remaining negative M_{ip} originates from the HL and SL magnetic moments that tend to align with the field at 10° from the out-of-plane direction. As the field decreases from negative saturation, both SL and HL moments rotate toward the out-of-plane easy anisotropy axis, such that at 0 Oe (ii) almost no in-plane component is left. Under positive field, a fraction of the ECC stack moments, mostly located inside the SL (as will be demonstrated in the following), rotate toward the field direction and the HL moments reverse, thus leading to the decrease in M_{pp} [Fig. 2(a)]. A maximum in-plane component is found around the coercive field (iii), where about half of the HL grains have switched. We therefore conclude that at (iii), the large M_{ip} signal originates mostly from a reversible tilt of the SL layer regions that are coupled to the not yet switched HL grains.

To quantify the rotation of the HL and SL magnetization during the reversal process, we perform a systemic study of the M_{ip} signal as a function of SL thickness [Fig. 3(a)]. We subtract the signal of the HL reference sample from each curve in order to separate out the SL reversal. This is referred to as the corrected SL signal. The evolution of the corrected M_{ip} at 12 kOe is plotted versus SL thickness (orange solid circle) in the inset of Fig. 3(b). A good agreement is obtained between this measured curve and the full SL magnetization

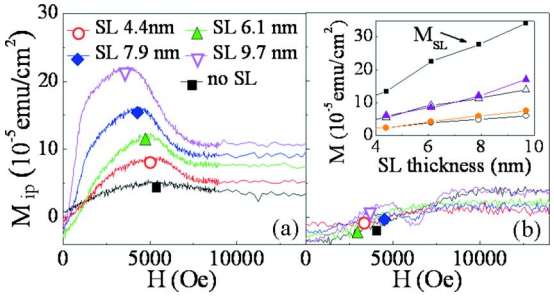

FIG. 3. (Color online) M_{ip} measured under a field (a) and at remanence (b) for samples with different SL thicknesses from 0 to 9.7 nm. The inset in (b) shows the SL moment areal density at saturation (black squares), the corrected M_{ip} at 12 kOe (orange circles) extracted from (a) and compared to $M_{SL}\sin(10°)$ (open circles), as well as the corrected M_{ip} maximum (violet solid triangles) extracted from (a) and compared to $\frac{1}{2}M_{SL}\sin(55°)$ (open triangles).

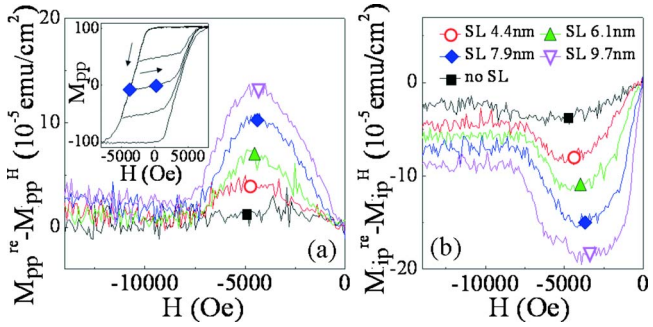

FIG. 4. (Color online) Difference between the moment signal at remanence (M_{re}) and under field (M_H) measured during a minor loop as a function of the field for both out-of-plane (a) and in-plane components (b), for different SL thicknesses. The inset in (a) represents an example of minor loops measured on the 7.9 nm SL sample.

expected at $10° \pm 2°$ tilt from the out-of-plane direction. The SL moment areal density at saturation M_{SL} is also plotted in the inset of Fig. 3(b). In addition, we plot the evolution of the corrected M_{ip} amplitude maximum versus SL thickness (violet triangle). This curve is well reproduced by assuming the magnetic configuration (iii) depicted in Fig. 2(b), i.e., by assuming that half of the SL magnetic moments are aligned already along their anisotropy axis pointing in the positive direction (switched grains) and half of the sample with SL moments forced at a large angle with respect to the easy out-of-plane axis (not yet switched grains). The open triangle curve in the inset of Fig. 3(b) that corresponds to $(M_{SL}/2)^*\sin(55°)$ is in close agreement with the evolution of the M_{ip} maximum from our experiments. It indicates that, when neglecting any moment rotation in the HL, the SL moments in the not yet reversed region are tilted at an average angle of around $55° \pm 5°$. Divergence arises for the thickest 9.7 nm SL sample, where the dipolar interaction as well as the strong lateral exchange may interfere most with the in-depth incoherent reversal. Moreover our simple model involves a coherent rotation in the depth of the SL, which is only expected for small SL thicknesses.[3]

Finally, in order to prove the reversibility of the moment rotation, we perform remanent M_{ip} and M_{pp} loops, i.e., after measuring in a field, we repeat the same measurement of M_{pp} and M_{ip} at zero field. As presented in Fig. 3(b), only a very weak signal is found at remanence, most probably from the HL. The M_{ip} signal, which we attribute to a rotation of the SL magnetic moment, is therefore purely reversible and directly responsible for the difference between H_c and H_{cr} in Fig. 1(c). This correlation is further confirmed by recording M_{ip} and M_{pp} during minor loops measured with the field at $\theta=10°$ [inset Fig. 4(a)]. The difference between the remanent and in-field M_{pp} and M_{ip} measured for a minor loop is shown in Figs. 4(a) and 4(b), respectively. It appears that the M_{pp} component of magnetization that is lost when returning to remanence is gained in the M_{ip} signal.[13] Here we clearly demonstrate that the slopes observed in the minor loops in the inset of Fig. 4(a) and previously reported in Refs. 11 and 7 originate from the reversible in-plane tilting of the magnetic moments.

In conclusion, we have grown a model ECC media without a SUL for a detailed study of the ECC reversal process. After optimizing the ECL, we increased the SL thickness thus inducing the common features of switching field reduction and increased incoherency of the reversal mechanism as compared to the single HL. The absence of the SUL allows directly measuring the in-plane component of the magnetization (M_{ip}) in the ECC stack during field reversal. A rudimentary model based on reversible rotation of the SL moments under field is used to understand our experimental results. Our work describes a new method to study and optimize the SL torque that can be used to improve recording performance of more complex structures, such as for example graded media.

[1]R. H. Victora and X. Shen, IEEE Trans. Magn. **41**, 2828 (2005).
[2]D. Suess, T. Schrefl, S. Fahler, M. Kirschner, G. Hrkac, F. Dorfbauer, and J. Fidler, Appl. Phys. Lett. **87**, 012504 (2005).
[3]D. Suess, J. Lee, J. Fidler, and T. Schrefl, J. Magn. Magn. Mater. **321**, 545 (2009), and references therein.
[4]H. N. Bertram and B. Lengsfield, IEEE Trans. Magn. **43**, 2145 (2007).
[5]J.-P. Wang, W. Shen, and J. Bai, IEEE Trans. Magn. **41**, 3181 (2005).
[6]T. Thomson, B. Lengsfield, H. Do, B.D. Terris, J. Appl. Phys. **103**, 07F548 (2008).
[7]H. S. Jung, E. M. T. Velu, S. S. Malhotra, G. Bertero, and U. Kwon, J. Magn. Magn. Mater. **320**, 3151 (2008), and references therein.
[8]A. Berger, N. Supper, Y. Ikeda, B. Lengsfield, A. Moser, and E. E. Fullerton, Appl. Phys. Lett. **93**, 122502 (2008).
[9]K. Tang, K. Takano, G. Choe, G. Wang, J. Zhang, X. Bian, and M. Mirzamaani, IEEE Trans. Magn. **44**, 3507 (2008).
[10]E. Girt, A. Yu. Dobin, B. Valcu, H. J. Richter, X. Wu, and T. P. Nolan, IEEE Trans. Magn. **43**, 2166 (2007).
[11]W. K. Shen and J.-P. Wang, J. Appl. Phys. **100**, 096113 (2006).
[12]H. Nemoto, I. Takekuma, H. Nakagawa, T. Ichihira, R. Arali, and Y. Hosoe, J. Magn. Magn. Mater. **320**, 3144 (2008).
[13]The difference in amplitude between the peaks in Figs. 4(a) and 4(b) originates from the fact that the M_{pp} and M_{ip} signal are projections of the tilted magnetization and therefore behave respectively as cosine and sine functions of the same angle.